Plastic behavior of nanophase Ni: A molecular dynamics computer simulation

H. Van Swygenhoven
Paul Scherrer Institut, 5232 Villigen PSI, Switzerland

A. Caro
Instituto Balseiro-Centro Atómico Bariloche, 8400 Bariloche, Argentina

We report molecular dynamics computer simulations of low temperature-high load plastic deformation of Ni nanophase samples with several mean grain sizes in the range of 3–5 nm. The samples are polycrystals nucleated from different seeds, with random location and orientation. Among the mechanisms responsible for the deformation, grain boundary sliding and motion, as well as grain rotation are identified. No dislocation activity is detected, in contrast to the behavior of coarse grain metals. Interpreting the results in terms of grain boundary viscosity, a linear dependence of strain rate with the inverse of the grain size is obtained. © *1997 American Institute of Physics.* [S0003-6951(97)03838-2]

Many of the distinctive properties of nanophase materials come from the large number of grain boundaries of nanophase materials compared to coarse grained polycrystals. In metallic systems, these phases exhibit mechanical properties which are controversial; in particular, a possible departure from the Hall–Petch behavior[1,2] has not yet been clearly established. Several mechanisms have been proposed to explain the deformation behavior based on the large number of triple junctions present, the lack of dislocation activity, grain boundary sliding, grain rotation, the presence of a softer phase in the boundaries, etc.[3–6]

Conventional physical models for crystal plasticity have been revisited in the literature to include size effects due to the presence of a large density of grain boundaries. The influence of these interfaces is crucial. While in conventional models of plasticity, interfaces represent obstacles for the deformation processes, contributing to the strengthening, in nanophase materials they are probably responsible for all of the observed plasticity.

Despite the continuously increasing body of experimental evidence, a definitive picture of plasticity in this new class of materials is still missing.

Large scale molecular dynamics computer simulations can help in the understanding of the relationship between grain boundary structure and overall properties. Approaches from different perspectives have led to different atomic modeling, ranging from the aggregation and consolidation of different randomly oriented clusters[7] to a deterministic aggregation of grains where position, shape, and orientation of each grain of the system is specified.[8] Between these approaches, samples have also been constructed by filling up an assigned volume with a polycrystal nucleating from different seeds[9] or by cooling down a liquid containing preoriented crystalline seeds.[10] Careful analysis of grain boundaries in computer generated nanosamples has been reported,[8] interpreting their structure in terms of amorphous regions.

Combining the concepts that the plastic activity is concentrated at the grain boundaries, and that these grain boundaries can be considered as amorphous regions, we naturally arrive at the picture of viscous plasticity in noncrystalline

materials. Previous reports on three-dimensional (3D) molecular dynamics simulations of wires showed grain boundary splitting and migration,[11] and experiments on Cu nanocrystals have determined pre-exponential factors and activation energies of finite temperature grain boundary viscosity, in terms of the misorientation between grains.[12]

In this work, we report 3-D results on computer simulations of plastic deformation of bulk nanoscale metallic samples: samples containing approximately 100 000 atoms each, with 15, 20, 25, and 50 grains (Ni_15,...Ni_50), which represent average grain sizes ranging from 3.4 to 5.2 nm, are constructed by filling the simulation cell volume with nanograins nucleated at random location and with random crystallographic orientation. Subsequently, those atoms in the grain boundaries closer than 2 Å to each other are removed. The samples are then relaxed to a minimum energy, using a parallel molecular dynamics code with a Finnis Sinclair potential in the Parrinello–Rahman approach, and periodic boundary conditions; details are given in Ref. 9. The final density of the samples at 0 K is in all cases above 97% of the perfect crystal value.

Other procedures to obtain relaxed samples, for example, annealing the as-created samples at high temperature, may lead to different structures and probably different plastic behavior. As for the real case, grain boundary structure is expected to be sensitive to the sample preparation procedure. These issues will be explored in future work.

Samples are then loaded and subsequently unloaded with an uniaxial stress of between 1 and 3 GPa, which is ~2% of the bulk modulus and below the range assumed for the theoretical strength of perfect crystals. Simulations were done under adiabatic conditions, in such a way that the mechanical work was converted into both heat and defect energy, which were then monitored. Despite the absence of a thermostat, the sample temperature in all runs was below 70 K after 10% deformation, for a starting temperature of 0 K. At these strain rates, no thermal gradients develop inside the sample. These stresses and temperature ranges gave us information on essentially *a*-thermal plastic deformation mechanisms.

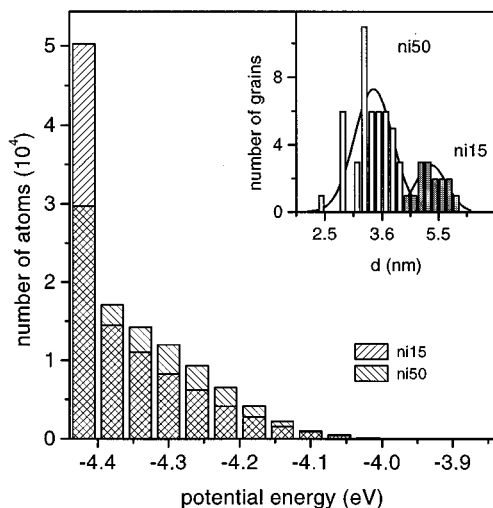Deformation has been followed using strain-time (creep)

FIG. 1. Histograms of potential energy of each atom for Ni_15 and Ni_50. Inset: Grain size distribution of Ni_50 and Ni_15, together with a log-normal fit, in a logarithmic x-axis scale.
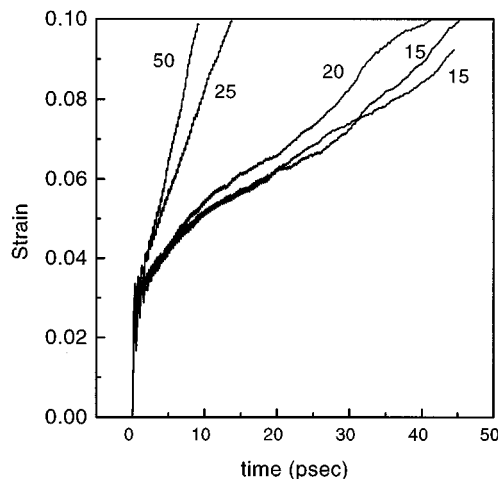

FIG. 2. Early stages of deformation vs time for samples with grain size between 3.2 (Ni_50) and 5.4 nm (Ni_15). Note the clear distinct between elastic and plastic components and the similarity with an ideal visco-elasto-plastic solid.

curves, visual inspection of slabs, and energy contour plots. Grain rotation has quantitatively been determined by Fourier transforming the atomic positions, and measuring the displacement of the diffraction spots on the Ewald sphere.

In Fig. 1, we show histograms of the potential energy per atom for the two extreme sizes, Ni_15 and Ni_50, in the undeformed state at 0 K. The relevance of the interfaces in terms of the number of atoms that have potential energy above the perfect crystal value can be clearly seen: 50% for Ni_15, and 70% for Ni_50, with 4.8 and 3.2 nm, respectively. If we count the atoms with an energy larger than the latent heat of melting (180 meV/atom for this potential), these numbers reduce to 12% and 18%, respectively. Figure 1 shows that the average potential energy of the defected atoms is comparable to the latent heat of melting, giving strong support to the interpretation of boundaries in terms of amorphous (or liquidlike) structures. Also shown in Fig. 1 is the grain size distributions for Ni_50 and Ni_15 with a logarithmic x axis, together with a log-normal distribution, which is the expected limit for a large number of grains.

Figure 2 shows the early stages of deformation for all samples. It becomes apparent that after an elastic contribution they show a linear behavior with an increasing strain rate for smaller grain sizes. A balance of the energy in terms of the work done by the stress gives: $\sigma \epsilon V = K_{th} + U_{th} + U_{def}$, where σ is the stress, ϵ the resultant plastic strain, V the cell volume, K_{th} and U_{th} the kinetic and potential contributions to thermal energy, and U_{def} the potential energy stored as defected atoms. Assuming $U_{th} = K_{th}$ (harmonic approximation), we can determine U_{def}; this procedure shows that 70% of the work performed on the sample by the external stress is transformed into heat, while 30% is stored as structural damage. This suggests that deformation takes place by increasing slightly the total number of defected atoms; a rough estimation of the number of atoms that become boundary atoms can be made by just dividing U_{def} by the average energy of a defected atom (the heat of melting). Evaluation at $\epsilon = 0.1$ indicates that the total amount of grain boundary increases by 13% during this process. This argu-

ment is further supported by the histograms of potential energy distribution, which remains similar before and after deformation, precluding the creation of a new type of defects or boundaries.

It is worth noticing that after relaxation after ultimate loading, the sample density recovers to 99% of the initial value, so one concludes that deformation takes place at a constant volume (i.e., no pore formation).

Some grains have been followed individually during deformation revealing the presence of several accommodation mechanisms. Grain boundary sliding in Ni_50 can be observed in Fig. 3 where the same section with thickness 1.8 Å, parallel to the xy plane of the sample, is shown before and after maximum loading. Grains 8 and 15 move relative to grain 6 in the direction of the uniaxial stress. Grains 8 and 15 keep their orientation, whereas several atoms of grain 6 take positions along other orientation of the adjacent grains. The interface between 6 and 15 remains sharp, but part of grain 6 rotates to accommodate deformation. The interface between grains 8 and 6 moves inside grain 6. This so called boundary motion is also observed in the upper part of grain 6 which has aligned itself to grain 1. Grain boundary motion can be the mechanism responsible for the formation of a planar interface between two or more grains, which after interaction with other planar interfaces allows easy gliding, as is suggested in Ref. 13.

Analysis of rotation of grain 1 in Ni_50 before and after loading indicates a rotation of the $\langle 100 \rangle$ axis towards $\langle 0, -1, -1 \rangle$ by 7.3° (see also Ref. 14); this rotation is comparable to the experimental determination by electron microscopy reported in Ref. 15.

As far as we have been able to detect, we have not seen any evidence of dislocation activity or crack formation, mechanisms that may lead to fracture.

These results show that deformation of fully dense nanophase metals at low temperature and high load occurs at constant volume and is due to grain boundary sliding, grain rotation, and grain boundary motion.

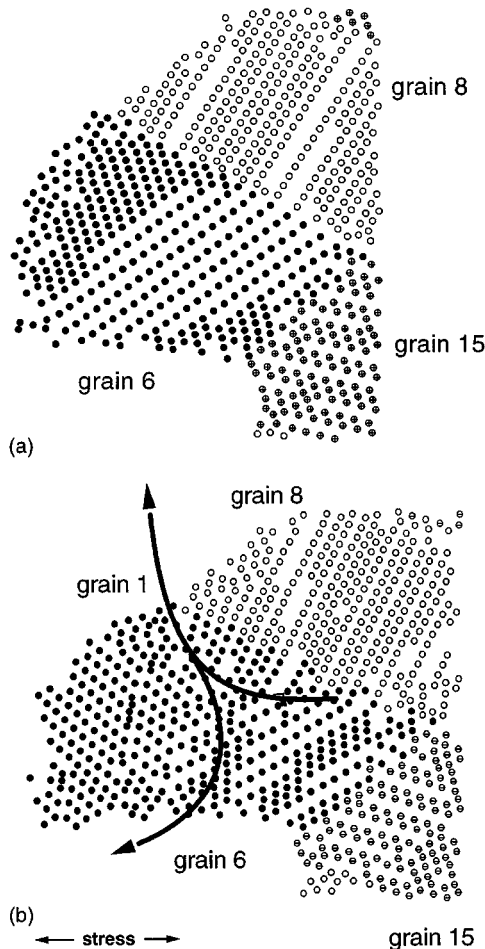Creep experiments are usually performed at high tem-

FIG. 4. Strain rate vs average grain diameter, together with a linear fit according to Eq. (1).

FIG. 3. Fraction of a slab showing selected grains of Ni_15. (a) before deformation; (b) after deformation. Different types of deformation mechanisms are identified, such as grain boundary motion and sliding.

peratures, where thermally activated migration of point defects at the interfaces or at the grains are the main source of plasticity. In our simulations at low temperature, diffusion is excluded; however we still observe that the major contribution comes from grain boundary a-thermal sliding, a viscous-like behavior.

To further explore this hypothesis of viscosity, we assume that these samples can be described simply as a linear elasto-visco-plastic solid.[16] By noting that in a sample with grain size d, the total surface per unit volume is proportional to d^{-1}, and also that the larger the interface area, the larger the number of slip channels that contribute to plastic deformations (like parallel dashpots in the visco-elasto-plastic model), we can write the following relation for the strain rate in the stationary state as a function of grain size

$$d\epsilon/dt = (1/d\beta)\sigma, \qquad (1)$$

where β characterizes the viscosity of a sample with $d = 1$ nm. Figure 4 shows strain rate versus d^{-1} obtained from the plastic region of Fig. 1, together with a linear fit representing Eq. (1). Although the offset at $d^{-1} = 0$ indicates that
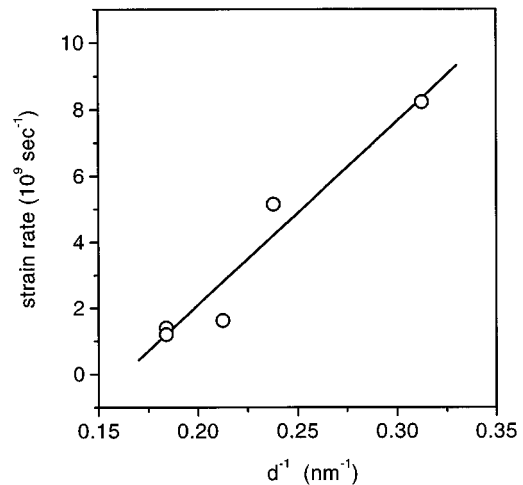
other mechanisms are probably present, this figure shows that the simple picture of linear viscous flow is qualitatively correct. We stress the fact that the small number of data points and their dispersion may hide a more complex dependence, but for the purpose of a first approach to the problem, linear viscosity is a reasonable simplifying assumption. The value $\beta = 1.5 \times 10^9$ Pa s/m^3 is predicted by this work.

In summary, we have shown that the mechanisms responsible for plastic deformation of nanocrystalline samples at low temperature and high stress are mainly viscous flow of interfaces, grain boundary motion, and grain rotation. No crack formation or dislocation emission is observed. Viscosity is expected to be strongly dependent on temperature and does not imply diffusion over long distances; it may become a mechanism competing with the Coble creep in the interpretation of the experimental data in the creep regime.

[1] E. O. Hall, Proc. Phys. Soc. London, Sect. B **64**, 747 (1951).
[2] N. J. Petch, J. Iron Steel Inst. **174**, 25 (1953).
[3] J. R. Weertman, Mater. Sci. Eng. A **166**, 161 (1993).
[4] V. Y. Gertsman, M. Hoffman, H. Gleiter, and R. Birringer, Acta Metall. Mater. **42**, 3539 (1994).
[5] R. W. Siegel and G. E. Fougere, Nanostruct. Mater. **6**, 205 (1995).
[6] Papers in ''Superplasticity in advanced Materials,'' ICSAM-94, Mater. Sci. Forum **170–172**, (1994).
[7] M. Celino, G. D'Agostino, and V. Rosato, Nanostruct. Mater. **6**, 751 (1995).
[8] D. Wolf, J. Wang, S. R. Phillpot, and H. Gleiter, Phys. Rev. Lett. **74**, 4686 (1995); S. R. Phillpot, D. Wolf, and H. Gleiter, J. Appl. Phys. **78**, 847 (1995).
[9] D'Agostino and H. Van Swygenhoven, Mater. Res. Soc. Symp. Proc. **400**, 293 (1996).
[10] Da Chen, Comput. Mater. Sci. **3**, 327 (1995).
[11] J. Schiotz, T. Rasmussen, K. W. Jacobsen, and O. H. Nielsen, Philos. Mag. Lett. **74**, 339 (1996).
[12] R. Monzen and T. Suzuki, Philos. Mag. Lett. **74**, 9 (1996).
[13] K. A. Padmanabhan, R. Nitsche, and H. Hahn, Proc. Euromat-95 (1995).
[14] H. Van Swygenhoven and A. Caro, Nanostruct. Mater. **9**, 669 (1997).
[15] M. Ke, S. A. Hackney, W. W. Milligan, and E. C. Aifantis, Nanostruct. Mater. **5**, 689 (1995).
[16] Y. M. Haddad, *Viscoelasticity of Engineering Materials* (Chapman and Hall, London, 1995).